DIPOLE MODE DETUNING IN THE NLC INJECTOR LINACS *

K.L.F. Bane, Z. Li, SLAC, Stanford University, Stanford, CA 94309, U.S.A.

1 INTRODUCTION

A major consideration in the design of the accelerator structures in the injector linacs of the JLC/NLC[1] is to keep the wakefield effects within tolerances for both the nominal (2.8 ns) and alternate (1.4 ns) bunch spacings. One important multi-bunch wakefield effect is beam break-up (BBU), where a jitter in injection conditions of a bunch train is amplified in the linac; another is static emittance growth caused by structure misalignments.

The injector linacs comprise the prelinac, the e^+ drive linac, the e^- booster, and the e^+ booster. The first three will operate at S-band, the last one, at L-band. Compared to the main (X–band) linac, the wakes will tend to be smaller by a factor $1/64$ and $1/512$, respectively, for the S– and L–band linacs. This reduction, however,—especially for the S-band machines—, by itself, is not sufficient. Two ways of reducing the wake effects further are to detune the first pass-band dipole modes and to damp them. In this report our goal is to design the accelerator structures for the injector linacs using detuning alone, an option that is simpler than including damping. We will consider only the effects of modes in the first dipole pass-band, whose strengths overwhelmingly dominate. The effects of the higher pass-band modes, however, will need to be addressed in the future. For a more detailed version of this work see Ref. [2]. Note that the design of the e^+ booster structure, which is straightforward, will not be discussed here.

Machine properties for the injector linacs are given in Table 1. Shown are the initial and final energies E_0, E_f, the machine length L, the initial (vertical) beta function averaged over a lattice cell $\bar{\beta}_0$, and the parameter ζ for a rough fitting of the beta function to $\bar{\beta} \sim E^{\zeta}$. The rf frequencies are sub–harmonics of 11.424 GHz. As for beam properties, for the nominal bunch train configuration (95 bunches spaced at 2.8 ns), the particles per bunch $N = 1.20$, 1.45, 1.45, 1.60×10^{10} and normalized emittance $\epsilon_{yn} = 3 \times 10^{-8}$, 10^{-4}, 10^{-4}, .06 rm, for the prelinac, e^+ drive, e^- booster, and e^+ booster, respectively. For the alternate configuration (190 bunches spaced at 1.4 ns) N is reduced by $1/\sqrt{2}$.

Table 1: Machine properties of the injector linacs.

Name	E_0, E_f [GeV]	L[m]	$\bar{\beta}_0$[m]	ζ
Prelinac	1.98, 10.0	558	8.6	1/2
e^+ Drive	0.08, 6.00	508	2.4	1/2
e^- Booster	0.08, 2.00	163	3.4	1/4
e^+ Booster	0.25, 2.00	184	1.5	1

* Work supported by the U.S. Department of Energy under contract DE-AC03-76SF00515.

2 EMITTANCE GROWTH

2.1 Beam Break-Up (BBU)

In analogy to *single-bunch* BBU in a linac[3], multi-bunch BBU can also be characterized by a strength parameter, but one dependent on bunch number m:

$$\Upsilon_m = \frac{e^2 N L S_m \bar{\beta}_0}{2E_0} g(E_f/E_0, \zeta) \qquad [m = 1, \ldots, M] \,, \tag{1}$$

with M the number of bunches in a train. The sum wake

$$S_m = \sum_{i=1}^{m-1} W[(m-i)\Delta t] \qquad [m = 1, \ldots, M] \,, \tag{2}$$

with W the transverse wakefield and Δt the time interval between bunches in a train. The wake, in turn, is given by a sum over the dipole modes in the accelerator structures:

$$W(t) = \sum_{n}^{N_m} 2k_n \sin(2\pi f_n t/c) \exp(-\pi f_n t/Q_n) \quad , \tag{3}$$

with t time and N_m the number of modes; f_n, k_n, and Q_n are, respectively, the frequency, the kick factor, and the quality factor of the n^{th} mode. The function $g(x)$ in Eq. 1 depends on the focusing profile in the linac. Assuming the beta function varies as $\bar{\beta} \sim E^{\zeta}$,

$$g(x, \zeta) = \frac{1}{\zeta} \left(\frac{x^{\zeta} - 1}{x - 1} \right) \qquad [\bar{\beta} \sim E^{\zeta}]. \tag{4}$$

If Υ_m, for all m, is not large, the linear approximation applies, and this parameter directly gives the (normalized) growth in amplitude of bunch m. The projected (normalized) emittance growth of the bunch train then becomes (assuming, for simplicity, that, in phase space, the beam ellipse is initially upright) $\delta\epsilon \approx \frac{1}{2} \Upsilon_{rms0}^2 y_0^2/\sigma_{y0}^2$, with Υ_{rms0} the rms with respect to 0 of the strength parameter, y_0 the initial bunch offset, and σ_{y0} the initial beam size. As jitter tolerance parameter, r_t, we can take that ratio y_0/σ_{y0} that yields a tolerable emittance growth, $\delta_{\epsilon t}$.

2.2 Misalignments

If the structures in the linac are (statically) misaligned with respect to a straight line, the beam at the end will have an increased projected emittance. If we have an ensemble of misaligned linacs then, to first order, the distribution in emittance growth at the end of these linacs is given by an exponential distribution $\exp[-\delta\epsilon/\langle\delta\epsilon\rangle]/\langle\delta\epsilon\rangle$, with[4]

$$\sqrt{\langle\delta\epsilon\rangle} = \frac{e^2 N L_a (x_a)_{rms} S_{rms}}{E_0} \sqrt{\frac{N_a \bar{\beta}_0}{2}}\, h(E_f/E_0, \zeta) \tag{5}$$

with L_a the structure length, $(x_a)_{rms}$ the rms of the structure misalignments, S_{rms} the rms of the sum wake *with respect to the average*, and N_a the number of structures; the function h is given by (again assuming $\bar{\beta} \sim E^{\zeta}$):

$$h(x,\zeta) = \sqrt{\frac{1}{\zeta x}\left(\frac{x^{\zeta}-1}{x-1}\right)} \qquad [\bar{\beta} \sim E^{\zeta}]. \quad (6)$$

Eq. 5 is valid assuming the so-called betratron term in the equation of motion is small compared to the misalignment term. We can define a misalignment tolerance: $x_{at} = (x_a)_{rms}\sqrt{\delta\epsilon_t/\langle\delta\epsilon\rangle}$, with $\delta\epsilon_t$ the tolerance in emittance growth.

We are also interested in the tolerance to cell-to-cell misalignments caused by fabrication errors. A structure is built as a collection of cups, one for each cell, that is brazed together, and there will be errors, small compared to the cell dimensions, in the straightness of each structure. To generate a wake (for a beam on-axis) in a structure with cell-to-cell misalignments we use a perturbation approach based on the eigenmodes of the unperturbed structure[5][2].

3 WAKEFIELD DESIGN

Reducing emittance growth requires reducing the sum wake. In the main (X-band) linac of the NLC, the strategy to do this is to use Gaussian detuning to generate a fast Gaussian fall-off in the wakefield envelope; in particular, at the position of the second bunch the wake is reduced by roughly 2 orders of magnitude from its initial value. At the lower frequencies of the injector linacs we have fewer oscillations between bunches and this strategy requires too much detuning. Instead, we will follow a strategy that puts early bunches on zero crossings of the wake, by a proper choice of the average frequency. As for the distribution of mode frequencies, we will aim for a uniform distribution, for which the wake is (for $\pi\bar{f}t/Q$ small):

$$W \approx \frac{2\bar{k}}{N_m}\sin(2\pi\bar{f}t)\,\frac{\sin(\pi\bar{f}t\Delta_{\delta f})}{\sin(\pi\bar{f}t\Delta_{\delta f}/N_m)} \quad , \quad (7)$$

with N_m the number of modes, $\bar{k}$ the average kick factor, $\bar{f}$ the average frequency, and $\Delta_{\delta f}$ the full width of the distribution. The wake envelope initially drops with t as a sinc function, but eventually resurges again, to a maximum at $t = N_m/(\bar{f}\Delta_{\delta f})$.

For the 2nd bunch to sit on the zero crossing requires that $\bar{f}\Delta t = n/2$, with n an integer. For S-band, given our implementation of the SLED-I pulse compression system, the optimal rf efficiency is obtained when the average dipole mode frequency is 4.012 GHz. For this case, with the alternate (1.4 ns) bunch spacing, $\bar{f}\Delta t = 5.62$. The half-integer is achieved by changing $\bar{f}$ by -2%, a change which, however, results in a net loss of 7% in accelerating gradient. One way of avoiding this loss is to reduce the group velocity by increasing the phase advance per cell of the fundamental mode from the nominal $2\pi/3$. In fact, we find that by going to $3\pi/4$ phase advance we can recapture this loss in gradient.

For the resurgence in the wake to occur after the bunch train has passed requires that $\Delta_{\delta f}$ be significantly less than $N_m/(M\bar{f}\Delta t)$, which, in our case, is about 10%. Another possibility for pushing the resurgence to larger t is to use two structure types, which can effectively double the number of modes available for detuning. This idea has been studied; it has been rejected in that it requires tight alignment tolerances between pairs of such structures.

3.1 Optimization

The cells in a structure are coupled to each other, and to obtain the wakefield we need to solve for the eigenmodes of the system. We obtain these numerically using a double-band circuit model [6]. The computer program we use generates $2N_c$ coupled mode frequencies f_n and kick factors k_n, with N_c the number of cells in a structure. It assumes the modes are trapped at the ends of the structure. We will use only the first N_c modes (those of the first pass-band) for our wakefield since they overwhelmingly dominate and since those of the second band are not obtained accurately.

The constants (circuit elements) for the program are obtained by fitting to results of a 2D electromagnetic program OMEGA2[7] applied to representative cell geometries, and then using interpolation. Here we consider structures of the disk–loaded type, with rounded irises. The iris and cavity radii are adjusted to give the correct fundamental mode frequency and the desired synchronous dipole mode frequency. Therefore, cell m can be specified by one free parameter, the synchronous frequency (of the first dipole mode pass-band). The $3\pi/4$ S-band structure consists of 102 cells with a cell period of 3.94 cm, iris thickness of 0.584 cm, and cavity radius ~ 4.2 cm; the Q due to wall losses (copper) $\sim 14,500$. Fig. 1 shows the first two dispersion curves of representative cell geometries (for iris radii from 1.30 to 2.00 cm). The plotting symbols give the OMEGA2 results, the curves, those of the circuit program.

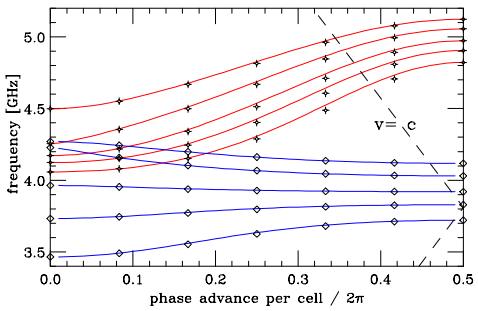

Figure 1: The dispersion curves of the first two dipole bands of representative cells in a $3\pi/4$ structure.

We will consider a uniform input (synchronous) frequency distribution, but with a slanting top. This leaves us with 3 parameters to vary: the (relative) shift in average frequency (from a nominal 4.012 GHz) $\delta\bar{f}$, the (relative) width of the distribution $\Delta_{\delta f}$, and the tilt parameter α ($-1 \le \alpha \le 1$, with $\alpha = 1$ giving a right triangle distribution with positive slope). Varying these parameters we calculate S_{rms0} and S_{rms} for the coupled modes, and for both

bunch train configurations, and we optimize. We find that a fairly optimal case consists of $\delta\bar{f} = -2.3\%$, $\Delta_{\delta f} = 5.8\%$, and $\alpha = -0.20$, where $S_{rms0} = S_{rms} = .004$ MV/nC/m^2. In Fig. 2 we show the dependence of S_{rms0} on $\delta\bar{f}$ and $\Delta_{\delta f}$ near the optimum.

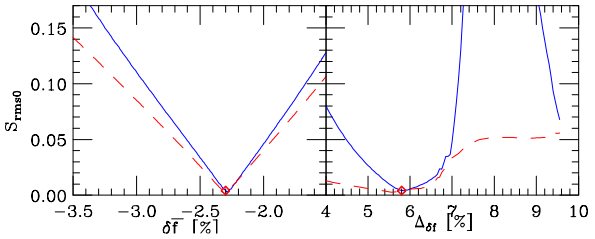

Figure 2: S_{rms0} [MV/nC/m^2] *vs.* $\delta\bar{f}$ and $\Delta_{\delta f}$ near optimum, for $\Delta t = 2.8$ ns (solid) and 1.4 ns (dashes).

In Fig. 3 we display, for the optimal case, the frequency distribution (a), the kick factors (b), and the envelope of the wake (c). The dashed curves in (a) and (b) give the synchronous (input) values. The plotting symbols in (c) give $|W|$ at the bunch positions for the alternate (1.4 ns) bunch train configuration. In (b) we see no spikes, thanks to the fact that the synchronous point is near pi, and, serendipitously, $f_0 < f_\pi$ for cell geometries near the beginning of the structure, $f_0 > f_\pi$ for those near the end[6]. (Note that for the optimized $2\pi/3$ structure, for which $f_0 > f_\pi$ for all cell geometries, there is such a spike, and consequently S_{rms0} is 5 times larger than here[2].) From (c) we note that many of the earlier bunches have wakes with amplitudes significantly below the wake envelope.

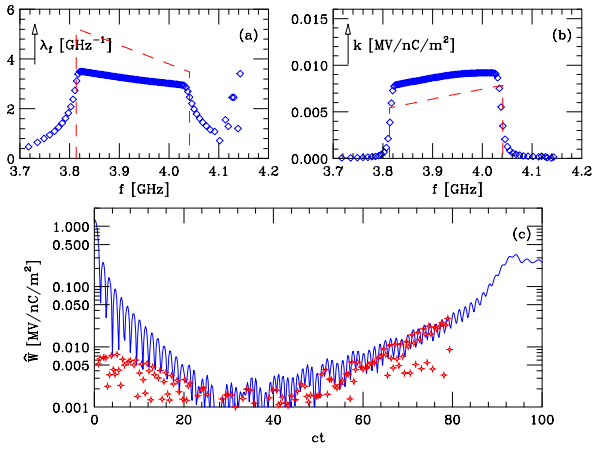

Figure 3: Results for the optimal $3\pi/4$ structure.

3.2 Frequency Errors

Errors in cell manufacturing will result in frequency errors. In Fig. 4 we give S_{rms0} and S_{rms}, when a random error component is added to the (input) synchronous frequencies of the optimal distribution (each plotting symbol, with its error bars, represents 400 seeds). With a frequency spacing of $\sim 8 \times 10^{-4}$, an rms frequency error of 1×10^{-4} is a relatively small perturbation, and for the 1.4 ns bunch spacing its effect is small, whereas for the 2.8 ns spacing it is not. The reason is that in the former case the beam sits on the half-integer resonance (which is benign), while in the latter case it sits on the integer (which is not)[2]. As to the effect in a linac, let us distinguish two types of errors: "systematic random" and "purely random" errors; by the former we mean errors, random in one structure, that are repeated in all structures of the linac; by the latter we mean random also from structure to structure. We expect the effect of a purely random error, of say, 10^{-4} (which we think is achievable) to be similar to a systematic random error of $10^{-4}/\sqrt{N_a}$. $N_a = 140$, 127, 41 in, respectively, the prelinac, the e^+ drive linac, and the e^- booster; therefore the appropriate abscissas in the figure become .8, .9, and 1.6×10^{-5}. At these points, for the 2.8 ns spacing, we see that S_{rms0} is only a factor 2 ± 1, 2 ± 1, 3 ± 2 times larger than the error-free result.

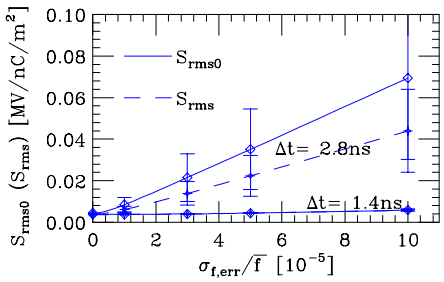

Figure 4: The effect of random frequency errors.

4 TOLERANCES

To obtain tolerances we performed particle tracking using LIAR[8] and compare the results with the analytical formulas given in Sec. 2. We take $\delta\epsilon_t = 10\%$ as acceptable. For BBU the tightest tolerance is for the e^+ booster, where r_t is 3.8 (2.2) analytically, 5.5 (3.0) numerically, for $\Delta t = 2.8$ (1.4) ns. For misalignments the tightest tolerance is for the prelinac, where x_{at} is 2.9 (4.6) mm analytically, 3.2 (4.8) mm numerically. (For the other machines these tolerances are $\gtrsim 10$ times looser.) Purely random machining errors, equivalent to 10^{-4} frequency errors, will tighten these results by 50-100%, but they are still very loose.

Finally, what is the random, cell-to-cell misalignment tolerance? Performing the perturbation calculation mentioned earlier for 1000 different random structures, we find that $S_{rms} = .27 \pm .12$ $(.032 \pm .003)$ MV/nC/m^2 for $\Delta t = 2.8$ (1.4) ns. We again see the effect of the integer resonance on the 2.8 ns option result. For the prelinac the cell-to-cell misalignment tolerance becomes 40 (600) μm for the 2.8 (1.4) ns configuration.

We thank T. Raubenheimer and attendees of the NLC linac meetings at SLAC for comments and suggestions.

5 REFERENCES

[1] NLC ZDR Design Report, SLAC Report 474, 589 (1996).
[2] K. Bane and Z. Li, SLAC-LCC-043, July 2000.
[3] A. Chao, "Physics of Collective Instabilities in High-Energy Accelerators", John Wiley & Sons, New York (1993).
[4] K. Bane, *et al*, EPAC94, London, England, 1994, p. 1114.
[5] R. M. Jones, *et al*, PAC99, New York, NY, 1999, p. 3474.
[6] K. Bane and R. Gluckstern, *Part. Accel.*, **42**, 123 (1994).
[7] X. Zhan, PhD Thesis, Stanford University, 1997.
[8] R. Assmann, *et al*, LIAR Manual, SLAC/AP-103, 1997.